Low-energy positron–nitrogen-molecule scattering: A rovibrational close-coupling study

T. Mukherjee[1,*] and M. Mukherjee[2]
[1]*Department of Physics, Bhairab Ganguly College, Kolkata 700056, India*
[2]*Saha Institute of Nuclear Physics, 1/AF Bidhannagar, Kolkata 700064, India*
(Received 18 March 2015; published 16 June 2015)

We study the positron–nitrogen-molecule scattering process under the rovibrational coupling method to include the effect of rotational and vibrational motion of the nuclei dynamically during the scattering process. Here we compute the angle integrated elastic and (state-to-state) rotational excitation, elastic and (state-to-state) vibrational (summed over rotational) excitation, and total (summed over rotational and vibrational) cross sections for the incident positron energy between 0.0 and 10 eV. However, in present paper we concentrate our discussion on the results in the lower-energy region, especially below 3.0 eV. To calculate the cross sections we use the model correlation polarization potential to include the distortion effect of the target electronic state in the presence of the positron. The calculated total cross sections are compared with the theoretical calculations and experimental results. The present theoretical results agree quite well with the recent theoretical and measured values. The vibrational and rotational elastic and excitation cross sections are also compared with the existing theoretical results. The state-to-state potential coupling and dynamical coupling effects on different cross sections are studied.

DOI: 10.1103/PhysRevA.91.062706 PACS number(s): 34.80.Bm

I. INTRODUCTION

Positron (electron) scattering with atoms or molecules is one of the important areas of research to study the nature of the interaction between subatomic particles [1–3]. In these scattering processes the projectile (positron or electron) and the electrons of the target atom or molecule interact via the Coulomb interaction. However, the theoretical quantum-mechanical study of these atomic or molecular systems involves the quantum-mechanical state of the target, which produces the so-called static and polarization potential. In the atomic case the electronic states of the atom produce the (electronic) state-to-state coupling potential. Under the close-coupling method these electronic coupling potentials act dynamically via a competitive process among the different channels when one solves the multichannel coupled differential equation in determining the scattering cross sections [4,5]. In the case of the molecular scattering process the nuclear motion (rotational and vibrational motion of the nuclei) takes part in the scattering dynamics in addition to the molecular electronic motion. Thus the theoretical quantum-mechanical calculation of the positron-molecule scattering process becomes complicated due to the inclusion of the nuclear dynamics. To tackle the problem several approximate methods have been used, such as fixed nuclei, adiabatic nuclei, adiabatic nuclei rotation, laboratory frame close-coupling (LFCC), body frame vibrational close-coupling (BFVCC), and rovibrational close-coupling (rovibrational LFCC) methods [6–10]. Among these the rovibrational close-coupling method is an elaborate and extensive way to include the rotational and vibrational motion of the nuclei in the calculation. Earlier this method was used to study positron–hydrogen-molecule scattering (see, e.g., [11]). In this method the total wave function of the projectile-target system is expanded in terms of electronic, rotational, and vibrational wave functions of the molecule. In the present work we study positron–nitrogen-molecule scattering using the rovibrational close-coupling method, keeping the molecule in its electronic ground state. Thus the electronic state effect appears here via the static and polarization potential like the atomic case. However, unlike the atomic case, in the molecular scattering process under the rovibrational coupling scheme (for the electronic ground state) one has to calculate the rotational and vibrational state-to-state potential, known as the rovibrational coupling potential. It should be noted that these coupling potentials include not only the rotational and vibrational states of the molecule but also the signature of the state of the projectile through the angular momentum coupling between the target and the projectile. Thus, in addition to the accurate determination of the potential, especially the polarization potential, one needs to concentrate on computing these coupling potentials for a theoretically accurate determination of the scattering cross sections. The calculation of the polarization potential for the molecular case is a crucial task that includes the distortion effect of the target electronic state in the presence of the projectile. Recently, Tenfen *et al.* [12] computed the *ab initio* correlation-polarization potential for the positron-target system, for different distances, following the approach proposed by Assafrao *et al.* [13] to get the scattering cross sections for positron–nitrogen-molecule scattering. They obtained fairly good results using this polarization potential when compared to the recent measurements. Although the calculation of the *ab initio* potential has to be used to get an accurate determination of the theoretical results, the determination of this potential is a very complicated task for any large system. Thus one has to rely on some approximate and reliable method to calculate this potential. One such model potential is the positron correlation-polarization potential (PCOP), specially designed for the positron as an incident particle. This model potential has been used in a number of scattering calculations to predict reliable results; see, e.g., those of Mukherjee and Sarkar [11], Mukherjee *et al.* [14], Gianturco and Mukherjee [15], Mazon *et al.* [16] and references therein. In the present calculation one of the motivations is to study the coupling effect of the rotational and vibrational state-to-state potentials

*Corresponding author: tapas.mukherjee1@gmail.com

on the scattering cross sections. In the present study we calculate state-to state coupling of the total potential (static plus correlation polarization) under the rovibrational coupling scheme using the PCOP. These close-coupling potentials are used in the solution of the (rotational and vibrational) close-coupled differential equation for the scattered multichannel positron wave function to study the effect of this dynamical coupling on scattering cross sections. We present here the total angle integrated cross sections (summed over rotational and vibrational cross sections), vibrational angle integrated elastic and excitation cross sections (summed over rotational cross sections), and rotational angle integrated cross section for vibrationally elastic processes. The present results are also compared with some of the existing theoretical and experimental results. It may be noted that at lower projectile energy the effect of the polarization potential becomes dominant, which is likely to give higher scattering cross sections as observed recently (discussed below). To verify the theoretical prediction and experimental observations we concentrate our discussion in the present study up to 3.0 eV.

II. THEORY

The theoretical scattering cross sections are calculated by solving the Schrödinger equation

$$(H - E)\Psi = 0 \tag{1}$$

with the usual scattering boundary conditions. Here H and Ψ are the total Hamiltonian and the total wave function of the positron molecule system. In the present case of positron–nitrogen-molecule scattering, using the (electronically elastic) rovibrational close-coupling method under the Born-Oppenheimer approximation, the total Hamiltonian H of the system is given by

$$H \equiv H(\vec{r}_p) + H_{el}(\vec{r}_e) + H_{\rm vib}(R) + H_{\rm rot}(\widehat{R}) + V_{p-{\rm mol}}(\vec{r}_p,\vec{r}_e,\vec{R}), \tag{2}$$

where $\vec{r}_p$ is the positron coordinate measured from the center of mass of the system; $\vec{r}_e$ collectively denotes the molecular electronic coordinates; $\vec{R}$ is the internuclear set of coordinates of the molecule; $H(\vec{r}_p)$ is the kinetic energy operator for the incident positron; $H_{\rm vib}(R)$, $H_{\rm rot}(\widehat{R})$, and $H_{el}(\vec{r}_e)$ are the vibrational, rotational, and electronic Hamiltonians of the target molecule, respectively; and $V_{p-{\rm mol}}(\vec{r}_p,\vec{r}_e,\vec{R})$ represents the positron-molecule interaction. The total wave function Ψ is characterized by, for the present method, the electronic, vibrational, and rotational quantum numbers of the molecule and the angular momentum quantum number of the projectile particle 0, v, j, and l, respectively, and is described by

$$\Psi^{JM}_{0vjl}(\vec{r}_p,\vec{r}_e,\vec{R}) = \chi_0(\vec{r}_e,\vec{R}) \sum_{\alpha''} r_p^{-1} u^{Jvjl}_{v'j'l'}(r_p) \times Y^{JM}_{j'l'}(\widehat{r}_p,\widehat{R})\varphi_{v'}(R), \tag{3}$$

where $\chi_0(\vec{r}_e,\vec{R})$ is the ground-state electronic wave function that parametrically depends on $\vec{R}$ and $\varphi_{v'}(R)$ is the vibrational wave function of the molecule. The angular basis function Y is given by

$$Y^{JM}_{j'l'}(\widehat{r}_p,\widehat{R}) = \sum_{m_j}\sum_{m_l} \langle jlm_jm_l|jlJM\rangle Y_{lm_l}(\widehat{r}_p)Y_{jm_j}(\widehat{R}). \tag{4}$$

The coefficients $\langle jlm_jm_l \mid jlJM\rangle$ are the familiar Clebsch-Gordan coefficients and $Y_{jm_j}(\widehat{R})$ and $Y_{lm_l}(\widehat{r}_p)$ are the nuclear rotational and positron angular wave functions, respectively. In this model $\vec{J} = \vec{j} + \vec{l}$ and its projection M along the nuclear axis are the good quantum numbers (constants of motion of the system). After substitution of the above equations into the Schrödinger equation (1) one gets the corresponding rovibrational close-coupled differential equation

$$\left(\frac{d^2}{dr^2_{r_p}} - \frac{l'(l'+1)}{r_p^2} + k^2_{\alpha\alpha'}\right)u^{Jjl}_{\alpha'}(r_p) = \sum_{\alpha''}\langle\alpha',J|V'(\vec{r}_p,\vec{R})|\alpha'',J\rangle u^{Jjl}_{\alpha''}(r_p), \tag{5}$$

where α collectively denotes the quantum numbers v,j,l,

$$V'(\vec{r}_p,\vec{R}) = \int \chi_0(\vec{r}_e,\vec{R})V_{p-{\rm mol}}(\vec{r}_p,\vec{r}_e,\vec{R})\chi_0(\vec{r}_e,\vec{R})d\vec{r}_e, \tag{6}$$

$$k^2_{jj'vv'} = 2(E - \varepsilon_{jj'} - \varepsilon_{vv'}), \tag{7}$$

with E is the incident positron energy and $\varepsilon_{jj'}$ and $\varepsilon_{vv'}$ the energy differences between rotational levels j and j' and the vibrational levels v and v', respectively.

The rotational and vibrational state-to-state coupling potential matrix elements used in the coupled equations are given by the relation

$$\langle v'j'l'|V'(\vec{r}_p,\vec{R})|v''j''l''\rangle = 2\iiint \varphi_{v'}(R)Y^{JM*}_{j'l'}(\widehat{r}_p,\widehat{R})V'(\vec{r}_p,\vec{R})\varphi_{v''}(R) \times Y^{JM}_{j''l''}(\widehat{r}_p,\widehat{R})dRd\widehat{R}d\widehat{r}_p. \tag{8}$$

Here the interaction potential has been expanded in terms of Legendre polynomials as

$$V'(\vec{r}_p,\vec{R}) = \sum_{\lambda} v_\lambda(r_p,R)P_\lambda(\widehat{r}_p,\widehat{R}). \tag{9}$$

Equation (8) takes the final form (after integration over the nuclear and projectile angular coordinates $\hat{R}$ and $\hat{r}_p$)

$$\langle v'j'l'|V'(\vec{r}_p,\vec{R})|v''j''l''\rangle = \sum_{\lambda}\langle v'(R)|v_\lambda(r_p,R)|v''(R)\rangle f_\lambda(j',l',j'',l'';J), \tag{10}$$

where $f_\lambda(j',l',j'',l'';J)$ is the angular coupling factor given by Lane and Geltman [17], which implies the angular coupling between rotational components (j,l) of initial and final states of the target and projectile

$$f_\lambda(j',l',j'',l'';J) = (-1)^{j'+j''-J}(2\lambda+1)^{-1}[(2j'+1) \times (2l'+1)(2j''+1)(2l''+1)]^{1/2} \times (l'l''00|l'l''\lambda0)(j'j''00|j'j''\lambda0) \times W(j'l'j''l'';J\lambda), \tag{11}$$

TABLE I. Vibrational and rotational threshold energies (in eV) for the nitrogen molecule. Here v and j label the vibrational and rotational quantum numbers, respectively.

$v=0$			$v=1$			$v=2$			$v=3$			$v=4$		
$j=0$	2	4	0	2	4	0	2	4	0	2	4	0	2	4
0.0	0.002	0.005	0.289	0.290	0.294	0.574	0.576	0.579	0.856	0.857	0.861	1.134	1.135	1.135

where $(ab00|ab\lambda 0)$ and $W(j'l'j''l'';J\lambda)$ are the familiar Clebsch-Gordan and Racah coefficients, respectively. In Eq. (10) the integration is over the nuclear coordinate R only.

As is evident from Eq. (10), to calculate the matrix element, one needs the vibrational wave functions of the molecule. These vibrational wave functions of the molecule are calculated using the differential equations

$$\left(\frac{d^2}{dR^2}+2\mu[\varepsilon_v-\varepsilon(R)]\right)\varphi_v(R)=0, \tag{12}$$

where μ is the reduced mass of the molecule and $\varepsilon(R)$ is electronic energy for different nuclear geometries that support the different vibrational bound states.

The interaction term $V_{p-\mathrm{mol}}(\vec{r}_p,\vec{r}_e,\vec{R})$ is the sum of two terms. One is the static term, which is calculated using the standard procedure. The well-known model PCOP, specially designed to describe the interaction between the positron and distorted molecule in the presence of the positron, is used to obtain the very important correlation-polarization potential. The details and its functional form are given elsewhere, viz., in [11].

The solution of rotationally and vibrationally coupled differential equations give the T-matrix elements $T^J(v'j'l',vjl)$ and using these elements we calculate the rotationally elastic and state-to-state integrated cross section (ICS) (angle integrated cross section), the vibrationally elastic and state-to state ICS (summed over the rotational ICS), and the total cross section (TCS) (summed over rotational and vibrational ICS). Besides these here we also calculate the quantity, the average vibrational energy transfer, defined as

$$\langle\Delta E_v\rangle=\frac{\sum_{v\neq 0}^{v'}\Delta E_{v\to v'}\sigma(v\to v')}{\sum_{v=0}^{v'}\sigma(v\to v')}. \tag{13}$$

This term describes the overall probability of transferring energy into the molecular degrees of freedom from a given initial level (here the vibrational level $v=0$).

III. COMPUTATIONAL DETAILS

To get the T-matrix elements and hence to calculate the cross sections the coupled differential equation (5) is solved using the variable-step-size Numerov method up to the radial distance of the positron $100a_0$ measured from the center of mass of the molecule. To obtain the potential matrix elements defined in Eqs. (6) and (7) one needs to know the ground-state electronic wave function $\chi_0(\vec{r}_e,\vec{R})$ and the vibrational wave function $\varphi_v(R)$. We have used Gaussian-type orbital expanded self-consistent-field electronic wave functions for 17 nuclear distances ranging from $1.4a_0$ to $7.5a_0$, which are the same as those used by Gianturco and Mukherjee [15]. The vibrational wave functions are obtained using Eq. (12). To get the converged cross sections the static potential is calculated up to the angular momenta $\lambda_{\max}=16$. The coupled differential equations are solved for the maximum vibrational states $v_{\max}=4$, the maximum rotational states $j_{\max}=4$, the maximum partial waves $l_{\max}=8$, and the maximum total quantum number $J_{\max}=4$. The maximum number of coupled equations solved is 45. In Table I we have tabulated the rotational and vibrational threshold energies for N_2.

IV. RESULTS AND DISCUSSION

In the present work we calculate the angle ICSs, viz., the elastic and (state-to-state) rotational, elastic, and (state-to-state) vibrational and TCSs for positron–nitrogen-molecule collisions. We compare our present results with the other theoretical and experimental results. Before studying the cross-section results we first present a discussion on the coupling potentials that play important roles in the scattering processes. There are two types of coupling that appear in the close-coupling method: potential coupling and dynamical coupling. The potential coupling is included via the terms $\langle v,j,l|v_\lambda|v',j',l'\rangle$ in the differential equation (5) (expressed in an elaborate form). The dynamical coupling effect appears in solving the coupled differential equation (5) where the solution of a particular channel depends on the influence of other channels. A number of coupling potentials appear in solving Eq. (5) whose number depends on the number of vibrational v and rotational j states of the molecule as well as the number of partial waves l considered. In Figs. 1 and 2 we plot such state-to-state potentials along with the other theoretically calculated values of Tenfen *et al.* [12] and Mazon *et al.* [16]. The present vibrationally elastic coupling potentials for two different moments (spherical and nonspherical components $\lambda=0,2$) $\langle 0,0,0|v_{0-\mathrm{tot}}|0,0,0\rangle$, $\langle 0,2,2|v_{0-\mathrm{tot}}|0,2,2\rangle$, $\langle 0,2,2|v_{2-\mathrm{tot}}|0,2,2\rangle$, and $\langle 0,2,2|v_{2-\mathrm{tot}}|0,2,2\rangle_{\mathrm{NRC}}$ are plotted in Fig. 1 [x-tot means the total (static plus polarization) potential and NRC implies that the angular coupling factor $f_\lambda(j',l',j'',l'';J)$ defined in Eqs. (10) and (11) is omitted from the summation]. By omitting this factor from the summation we effectively ignore the angular coupling. It may be noted that the no-rotational-coupling data shown here are for comparison only and are not used in the present calculation. As the nitrogen molecule is a homonuclear diatomic molecule, only even values of the j, l, and λ components for potentials are nonzero. Figure 1 shows that the variation of the spherical components of the potential with the distance is almost the same in nature, although the magnitudes differ from each other. It should be noted that the correlation-polarization potential used in the present calculation and used by Mazon *et al.* [16] is the same (the PCOP) and both calculations consider the

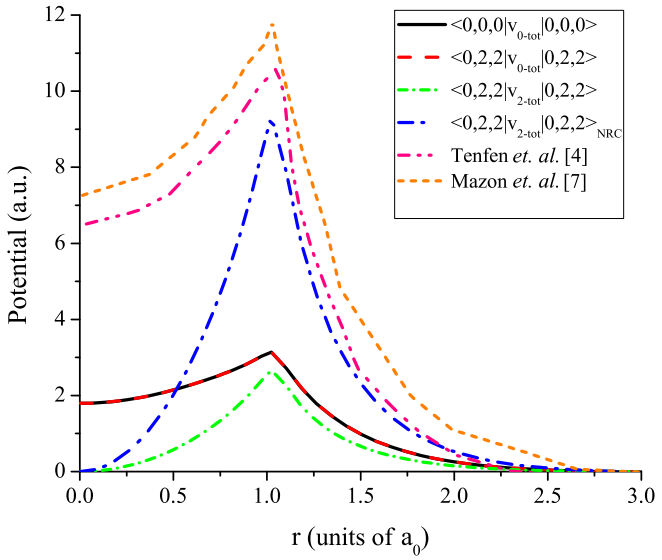

FIG. 1. (Color online) Present computed rovibrational state-to-state coupling potentials for spherical and non-spherical ($\lambda = 0,2$) components along with the other theoretical results. The potential matrix elements are defined in the text.

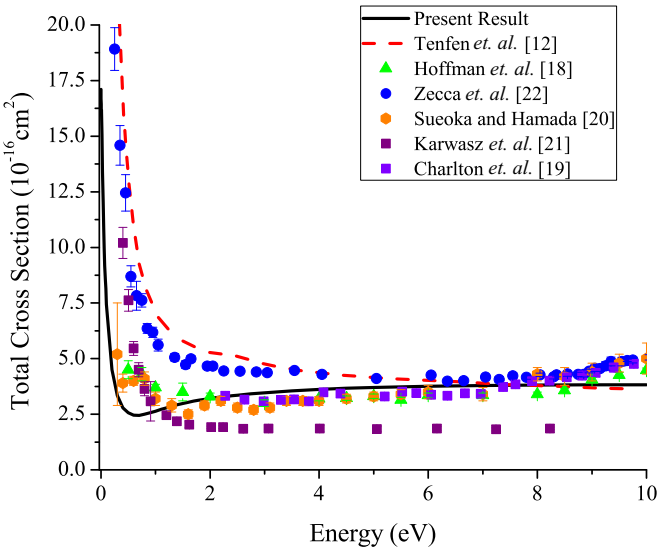

FIG. 3. (Color online) Comparison between present computed angle integrated total cross sections and the theoretical results of Tenfen *et al.* and different measured values for positron–nitrogen-molecule scattering.

vibrational excitation processes. Thus the calculated spherical component of the potential by Mazon *et al.* is nearly the same as the present $\langle 0,2,2|v_{2-\mathrm{tot}}|0,2,2\rangle_{\mathrm{NRC}}$ component as this has no angular dependence or rotational angular momentum coupling. However, the small difference may be attributed to the use of different vibrational wave functions in computing the coupling potentials. The difference between the potentials calculated by Tenfen *et al.* [12] and the present one is due to the use of a different correlation-polarization potential. For comparison, in Fig. 1 we also plot the component $\langle 0,2,2|v_{0-\mathrm{tot}}|0,2,2\rangle$. From the figure it is evident that the magnitude of this component is the same as that of the component $\langle 0,0,0|v_{0-\mathrm{tot}}|0,0,0\rangle$ (the two graphs merge with each other), although j and l differ as no angular factor appears for $\lambda = 0$. Another very interesting result is seen when we compare the $\langle 0,2,2|v_{2-\mathrm{tot}}|0,2,2\rangle$ and $\langle 0,2,2|v_{2-\mathrm{tot}}|0,2,2\rangle_{\mathrm{NRC}}$ components. They show that inclusion of rotational coupling makes the final effective potential less repulsive for positron-molecule collisions, which affects the cross-section results. In Fig. 2 we present two other coupling potentials $\langle 0,2,2|v_{2-\mathrm{tot}}|0,2,2\rangle$ and $\langle 0,4,4|v_{2-\mathrm{tot}}|0,4,4\rangle$, two nonspherical components of the potential. This figure shows that the nature of variation of the two components is the same and the magnitudes are also comparable. This indicates that, although the scattering probability for the $j = 4$ state may be less than that for the $j = 2$ state, with $j = 4$ being the higher excited state, the coupling effect of the higher excited states in the scattering dynamics on the other probabilities is not to be ignored.

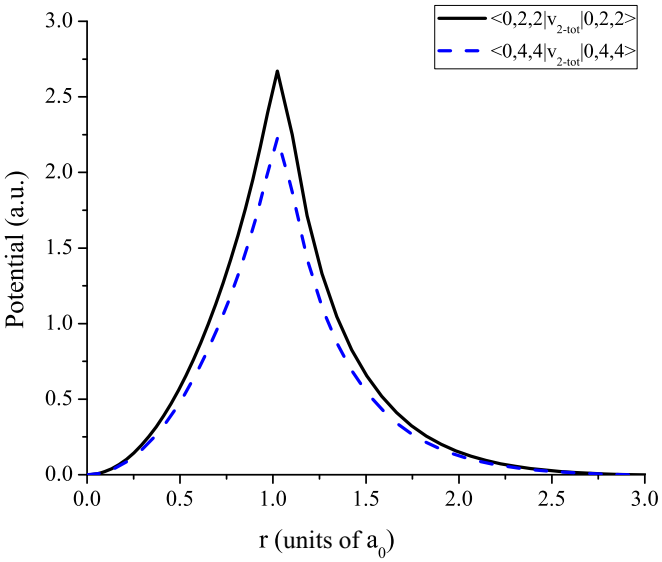

FIG. 2. (Color online) Present computed rovibrational state-to-state coupling potentials for nonspherical ($\lambda = 2$) components. The potential matrix elements are defined in the text.

In Fig. 3 we plot the present computed angle integrated total (summed over rotational and vibrational) cross sections with the experimental results of Hoffman *et al.* [18], Charlton *et al.* [19], Sueoka and Hamada [20], Karwasz *et al.* [21], and Zecca *et al.* [22] up to 10.0 eV. In this figure the calculated result of Tenfen *et al.* [12] is also included for comparison. The figure shows that the present result is in very good agreement with the measured values above about 2.0 eV. It can be seen that the measured cross sections differ from each other substantially in the lower-energy region, i.e., below 3.0 eV. Zecca *et al.* attributed the difference of their results with the other measured values to the superior angular resolution of their apparatus compared to those of other measurements. Tenfen *et al.* [12] compared their result with the previously calculated results and experimental values. Their results are in close agreement with the recently measured values of Zecca *et al.* They attributed this agreement to the fairly described *ab initio* target polarization potential. In the present calculation we do not use any such *ab initio* potential, but have used the so-called model correlation polarization potential, like the PCOP in the framework of the

rovibrational close-coupling scheme. However, it is interesting to note that the trend of the present result, especially in the lower-energy region, matches well with the results of Tenfen *et al.* and Zecca *et al.* except for the appearance of a minimum in the present result. Tenfen *et al.* in their paper discussed the utility of using an *ab initio* potential over the model potential like the PCOP in determining the scattering cross sections. In their discussion they pointed out the important differences in the construction of *ab initio* and model potentials. These are mainly (i) the choice of cutoff radius and (ii) the consideration of the target molecule as a free-electron gas in the presence of a positron to construct the PCOP. In the present calculation, as we are using the PCOP, the effect of the choice of cutoff radius may give rise to the minimum in the computed cross section shown in Fig 3. However, in the present rovibrational close-coupling formalism the target effect appears through the inclusion of (nuclear) state-to-state coupling. The larger values of the cross sections obtained by Tenfen *et al.* are due to the use of the *ab initio* polarization potential, which includes the target distortion effect and produces a more attractive polarization potential than the other polarization potential used. To calculate this potential Tenfen *et al.* took the distorted target molecule and calculated the electronic wave function, which depends parametrically on the nuclear coordinates. Thus their calculated distortion potential is electronic in nature where the effect of the nuclear degree of freedom is included parametrically. On the other hand, the present calculation includes the distortion of the target under the model PCOP and that of the nuclear motion dynamically under the rovibrational coupling scheme whose collective effect makes the potential less repulsive and produces the higher cross sections comparable to the theoretical results of Tenfen *et al.* and measured values especially in the lower-energy region.

In Fig. 4 we plot the present calculated TCS along with some of the theoretically calculated results, viz., the results by Elza *et al.* [23] including nonadiabatic (correlation) effects, the *R*-matrix calculation result of Danby and Tennyson [24], and the results using the Schwinger multichannel calculation (SMC) by Carvalho *et al.* [25] as well as the values of Tenfen *et al.* [12]. One of the motivations of the present work is to study the importance of the coupling effect of nuclear motion on the total scattering process, especially in the lower-energy region where the positron spends much time interacting with the target molecule. To show this nuclear effect, in Fig. 4 we also plot the values calculated using the BFVCC approximation [15] and the method of continued fractions (MCF) [16] extended to vibrational excitation processes by Mazon *et al.* From the figure it is evident that the results obtained by Tenfen *et al.* are higher compared to all other theoretical data presented in the figure and the reason for this is explained by them as due to the effect of the long-range interaction potential. The figure also shows that the present results lie between all the theoretical numbers. This reflects the fact that the state-to-state coupling effect gives rise to a stronger effective potential, resulting in a higher cross section than the data obtained using the BFVCC method, the MCF, and the *R*-matrix method. However, this effective potential is not strong enough to give the high values as obtained using the SMC and nonadiabatic (correlation) processes. It should be noted that the BFVCC and MCF calculations use the same model PCOP. Moreover, these two studies have included the vibrational dynamics in their calculations but solved with different methods, whereas the present calculation includes the rotational motion of the nuclei along with the vibrational motion. From Fig. 4 it is evident that the two previously calculated values are almost the same, as they should be, but the present values are higher. In the present rovibrational close-coupling method the coupling between the projectile and the target molecule, which happens to be effective through the angular momentum coupling (coupling between the nuclear rotational angular momentum $\vec{j}$ and the projectile angular momentum $\vec{l}$ giving total angular momentum $\vec{J} = \vec{j} + \vec{l}$), appears to be attractive. Thus, in the present case of the positron-molecule collision the net scattering potential becomes less repulsive and bears the reason behind the higher value of the cross section compared to the BFVCC and MCF results.

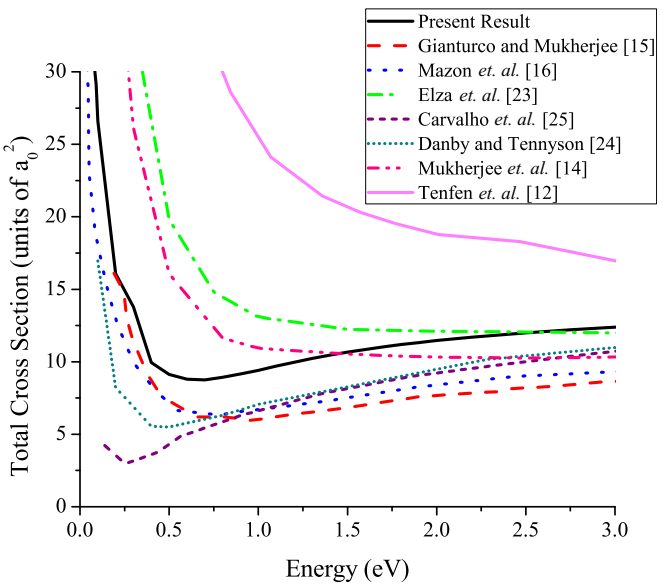

FIG. 4. (Color online) Comparison between present computed angle integrated total cross sections and the other theoretical results for positron–nitrogen-molecule scattering.

In Figs. 5–7 the present vibrational angle integrated excitation cross sections (vibrational ICSs) for the vibrational $0 \rightarrow 1$, $0 \rightarrow 2$, and $0 \rightarrow 3$ (summed over rotational states) transition processes, respectively, are plotted along with the theoretical BFVCC result of Gianturco and Mukherjee [15] and the MCF result of Mazon *et al.* [16]. Figures 5–7 show that the values of the excitation cross sections are much less than the total cross sections (Fig. 1, dominated by the elastic cross section). Moreover, the $0 \rightarrow 2$ and $0 \rightarrow 3$ cross sections are also two orders fewer than the $0 \rightarrow 1$ cross section. Although the numerical values are small, some interesting features regarding the coupling effect can be seen from the results. It is evident from Figs. 5 and 6 that the present $0 \rightarrow 1$ and $0 \rightarrow 2$ cross sections are higher than the results of Mazon *et al.* The reason behind this is the effect of the potential coupling where a reduction of the effective repulsive scattering potential happens due to the rotational coupling effect as discussed earlier. This effect also can be seen from Figs. 6 and 7 when the present $0 \rightarrow 2$ and $0 \rightarrow 3$ cross sections are

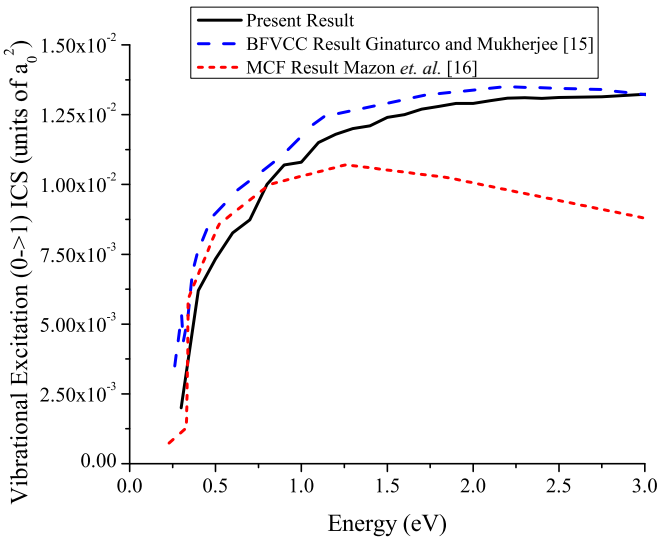

FIG. 5. (Color online) Comparison between present computed angle integrated vibrational state-to-state $0 \rightarrow 1$ excitation cross sections and the other theoretical results for positron–nitrogen-molecule scattering.

compared with the BFVCC and MCF results. However, the interesting result can be seen from Fig. 5 when we compare the present $0 \rightarrow 1$ cross section to the BFVCC cross section: The two results are very much comparable to each other in the lower-energy region, with the BFVCC result being a little higher than the present value. The present data include both rotational and vibrational motion of the molecule, whereas the BFVCC calculations include only the vibrational motion. The two comparable results indicate that here the dynamical coupling effect is more dominant than the potential coupling effect. Here the vibrational dynamics affects the transition probability at least for the $0 \rightarrow 1$ channel exceeding the effect of the rotational coupling effect. However, in the cases of $0 \rightarrow 2$ and $0 \rightarrow 3$ channels this dynamical effect seems to

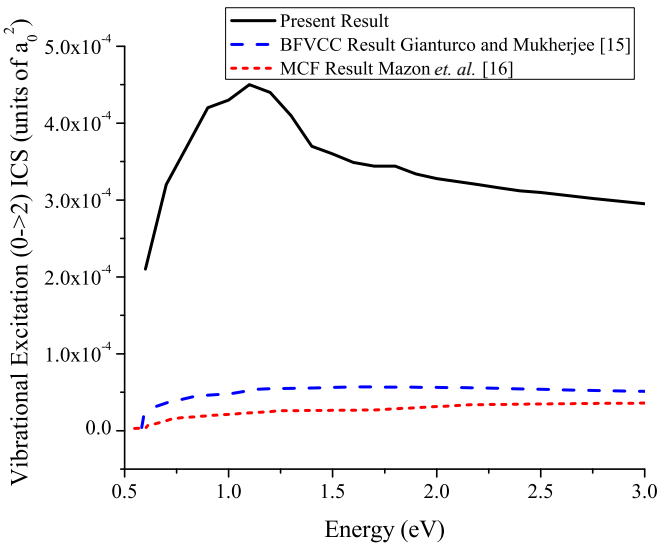

FIG. 6. (Color online) Same as Fig. 5 but for $0 \rightarrow 2$ excitation cross sections.

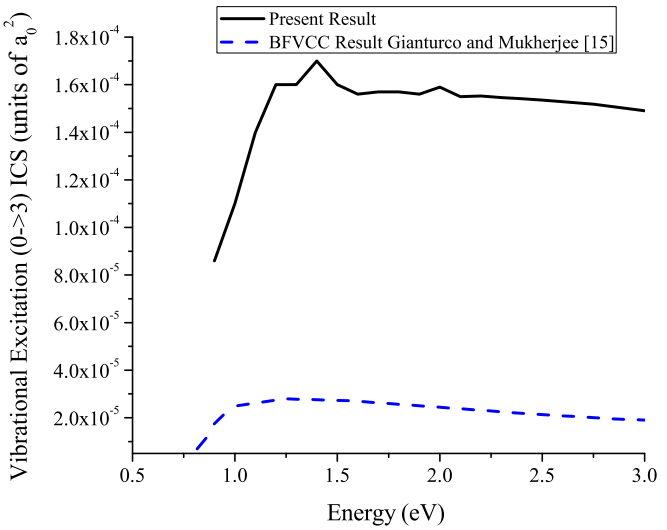

FIG. 7. (Color online) Same as Fig. 5 but for $0 \rightarrow 3$ excitation cross sections.

be less effective compared to the potential effect. We feel that the competition between these two coupling effects could be studied more elaborately if measured data for state-to-state vibrational excitation cross sections as well as other theoretical calculations were available.

Here we also calculate the rotational angle integrated cross sections for both elastic and excitation processes. In Fig. 8 we plot the rotational elastic $0 \rightarrow 0$ and inelastic $0 \rightarrow 2$ processes for the vibrationally elastic (vibrational $0 \rightarrow 0$) channel. The figure shows that in the lower-energy region both cross sections are comparable to each other, whereas in the higher-energy region the elastic cross section is larger. Like the vibrational excitation process, as there are no measured values of rotational cross sections, we compare our present rotational $0 \rightarrow 0$ and $0 \rightarrow 2$ results with the calculated values of rotational LFCC

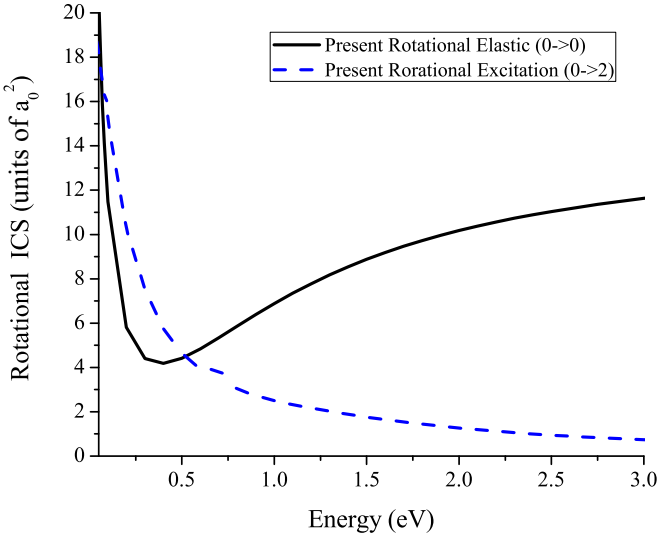

FIG. 8. (Color online) Present computed angle integrated rotational state-to-state (for vibrational elastic $0 \rightarrow 0$) $0 \rightarrow 0$ (elastic) and $0 \rightarrow 2$ (excitation) cross sections for positron–nitrogen-molecule scattering.

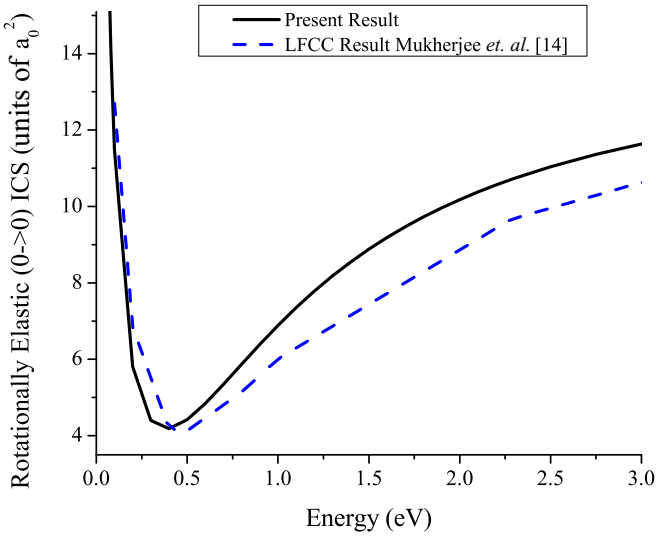

FIG. 9. (Color online) Comparison between present computed angle integrated rotational state-to-state $0 \rightarrow 0$ (elastic) (for vibrational elastic $0 \rightarrow 0$) cross sections with other theoretical result for positron–nitrogen-molecule scattering.

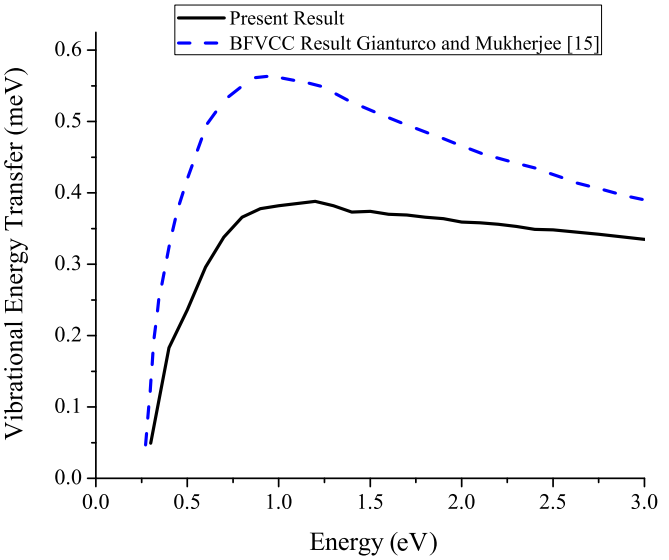

FIG. 11. (Color online) Comparison between present computed average vibrational energy transfers as defined in Eq. (13) with other theoretical result for positron–nitrogen-molecule scattering.

using the same PCOP result of Mukherjee *et al.* [14] in Figs. 9 and 10, respectively. We see from both figures that the present results are higher than the rotational LFCC result except in the very-low-energy region. As both calculations involve the same rotational coupling, the responsibility for the different result may be attributed to the vibrational coupling effect. Thus the present higher values of the cross sections indicate that the vibrational coupling (potential or dynamical) effectively reduces the repulsive potential over the rotational coupling. However, which coupling effect plays the dominant role over the other is not clear from these data. More calculations and measurements are necessary to resolve this issue.

Finally, in Fig. 11 we present the vibrational energy transfer defined by the relation (13) along with the BFVCC result [15]. From the figure it can be seen that the nature of the variation with the energy is the same for both cases: The BFVCC values are higher in the lower-energy range and coalesce with each other for the higher-energy values. The lower values of the present results are due to the lower values of the present vibrational $0 \rightarrow 1$ excitation cross section than the BFVCC cross section, especially in the lower-energy region. Moreover, the higher values of the rotationally uncoupled BFVCC result over the present rovibrationally coupled result show the same trend of higher values of the decoupled BFVCC adiabatic angular momentum coupling result over the vibrationally coupled result as demonstrated by Gianturco and Mukherjee [15]. The higher values of energy transfer using the decoupled scheme show that the efficiency of energy transfer into the molecular degree of freedom by the impinging positron depends on the coupling effect and hence the reduction of the effective scattering potential.

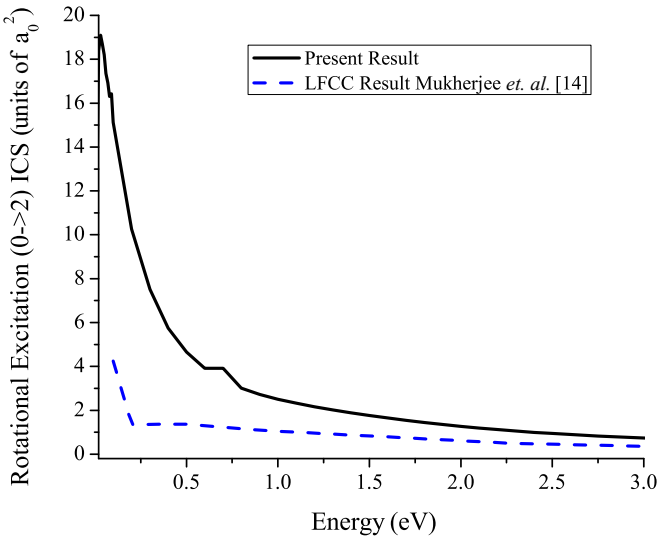

FIG. 10. (Color online) Same as Fig. 9 but for rotational $0 \rightarrow 2$ excitation cross sections.

V. CONCLUSION

In the present work we reported the angle integrated rotationally elastic and (state-to-state) excitation, vibrational elastic and (state-to-state) excitation (summed over rotational), and total (summed over vibrational and rotational) cross sections for positron–nitrogen-molecule scattering up to 3.0 eV of incident positron energy under the rovibrational close-coupling method. However, the total-cross-section results were plotted up to 10.0 eV to compare the present data with the different measured values. The rovibrational coupling method is an extensive technique used to study the molecular scattering processes that take into account the rotational and vibrational motion of the nuclei in a dynamical way. Under the static polarization approximation, where the ground electronic state of the molecule is considered, the distortion of the target can be included via the model correlation polarization potential. Here to compute the cross sections we used the

model correlation-polarization potential (the PCOP) specially designed for the positron as the incident particle. Besides this, under the rovibrational close-coupling framework, the rovibrational state-to-state potential coupling and the dynamical coupling due to the rotational and vibrational motion of the nuclei were also included in the determination of the scattering cross sections. We compared our present total cross sections with the theoretical calculations of Tenfen *et al.* [12] and with other measured values [18–22]. The very interesting observation is that the present result almost matches the theoretical values as well as the measured values, specifically in the lower-energy region, although the two theoretical values use a different kind of polarization potential. It seems that the enhanced cross section in the lower-energy region is due to the reduction of the effective repulsive scattering potential. In the present case the reduction of the scattering potential is due to the rotational coupling effect explained before, whereas the calculation of Tenfen *et al.* [12] shows that the reason lies with the use of the *ab initio* target polarization potential. The effect of the potential coupling was also explained by comparing the present total cross section with the theoretical calculations by Tenfen *et al.* (using *ab initio* target polarization) [12], Gianturco and Mukherjee (BFVCC) [15], Mazon *et al.* (vibrational MCF) [16], Elza *et al.* (nonadiabatic correlation) [23], Danby and Tennyson (*R*-matrix method) [24], and Carvalho *et al.* (SMC) [25]. We also compared the present vibrational and rotational cross sections with the LFCC calculation of Mukherjee *et al.* [14] and the above two theoretical calculations up to 3.0 eV. From these comparisons we found the importance of the dynamical coupling effect on the scattering process. As there are no measured values for the nuclear excitation processes, we were unable to make any specific comments on the coupling effects. Finally, we showed the vibrational energy transfer using the present rotationally coupled formalism and compared it with the rotationally decoupled BFVCC result of Gianturco and Mukherjee. This also demonstrates the importance of the coupling effect due to nuclear motion in the molecular scattering process. However, so far, as far as the total-cross-section results are concerned, we feel that further investigation is necessary to find the reason behind the matching of the results of the present coupled calculation with the model polarization potential and those of the decoupled calculation using the *ab initio* polarization potential.

[1] N. F. Lane, Rev. Mod. Phys. **52**, 29 (1980).
[2] A. S. Ghosh, N. C. Sil, and P. Mandal, Phys. Rep. **87**, 313 (1982).
[3] E. A. G. Armour, Phys. Rep. **169**, 1 (1988).
[4] M. Mukherjee, M. Basu, and A. S. Ghosh, J. Phys. B **23**, 757 (1990).
[5] M. Mukherjee, T. Mukherjee, and A. S. Ghosh, J. Phys. B **24**, L463 (1991).
[6] M. A. Arthurs and A. Dalgarno, Proc. R. Soc. London Ser. A **256**, 560 (1960).
[7] A. Temkin and K. V. Vasavada, Phys. Rev. **160**, 109 (1967).
[8] A. Temkin and F. H. M. Faisal, Phys. Rev. A **3**, 520 (1971).
[9] A. N. Feldt and M. A. Morrison, J. Phys. B **15**, 301 (1982).
[10] A. S. Ghosh and T. Mukherjee, Can. J. Phys. **74**, 420 (1996).
[11] T. Mukherjee and N. K. Sarkar, J. Phys. B **41**, 125201 (2008).
[12] W. Tenfen, K. T. Mazon, S. E. Michelin, and F. Arretche, Phys. Rev. A **86**, 042706 (2012).
[13] D. Assafrao, H. R. Walters, F. Arretche, A. Dutra, and J. R. Mohallem, Phys. Rev. A **84**, 022713 (2011).
[14] T. Mukherjee, A. S. Ghosh, and A. Jain, Phys. Rev. A **43**, 2538 (1991).
[15] F. A. Gianturco and T. Mukherjee, Phys. Rev. A **55**, 1044 (1997).
[16] K. T. Mazon, W. Tenfen, S. Michelin, F. Arretche, M.-T. Lee, and M. M. Fujimoto, Phys. Rev. A **82**, 032704 (2010).
[17] N. F. Lane and S. Geltman, Phys. Rev. **160**, 53 (1967).
[18] K. R. Hoffman, M. S. Dababneh, Y. F. Hsieh, W. E Kauppila, V. Pol, J. H. Smart, and T. S. Stein, Phys. Rev. A **25**, 1393 (1982).
[19] M. Charlton, T. C. Griffith, G. R. Heyland, and G. L. Wright, J. Phys. B **16**, 323 (1983).
[20] O. Sueoka and A. Hamada, J. Phys. Soc. Jpn. **62**, 2669 (1993).
[21] G. P. Karwasz, D. Plizska, and R. S. Brusa, Nucl. Instrum. Methods Phys. Res. Sect. B **247**, 68 (2006).
[22] A. Zecca, L. Chiari, A. Sarkar, and M. Brunger, New J. Phys. **13**, 115001 (2011).
[23] B. K. Elza, T. L. Gibson, M. A. Morrison, and B. C. Saha, J. Phys. B **22**, 113 (1989).
[24] G. Danby and J. Tennyson, J. Phys. B **24**, 3517 (1991).
[25] R. C. Carvalho, M. T. do N. Varella, M. A. P. Lima, E. P. Silva, and J. S. E. Germano, Nucl. Instrum. Methods Phys. Res. Sect. B **171**, 33 (2000).